ELSEVIER

International Journal of Heat and Fluid Flow 21 (2000) 285–290

International Journal of HEAT AND FLUID FLOW

www.elsevier.com/locate/ijhff

Experimental investigation of turbulent wake–blade interaction in axial compressors

A. Sentker *, W. Riess

Institute for Turbomachinery, University of Hannover, Appelstr. 9, 30167 Hannover, Germany

Received 27 August 1999; accepted 1 February 2000

Abstract

The fundamentally unsteady character of flow in multi-stage turbomachines is traditionally neglected in most of the flow calculation methods. The rapid development of hard- and software for numerical flow simulation has opened possibilities for investigation of the unsteady flow in turbomachines. The still existing methodical problems in the simulation especially of turbulent flow makes the experimental validation of numerical results indispensable. In a low-speed research axial compressor with incompressible flow conditions and relatively large geometric dimensions, a flow measuring system based on split-film probes has been installed and extensively operated. Measurements of the unsteady flow field and the turbulence properties concerning the blade wakes have been made and reported. In the subsequent investigation, the passage of the IGV wakes and the rotor blade wakes of the first rotor through the adjacent stator blade row have been explored in one measuring plane in front of the stator, four measuring planes within the stator and a measuring plane behind the stator at the mean radius of the blading. Measurements of the unsteady absolute velocity field in the S1-plane and the turbulent fluctuations have been made. The transportation of the IGV wake through the stator is one result of the measurements. The decay of the fluctuation components inside the stator blade row has been investigated in detail.

Keywords: Low-speed axial compressor; Wake transport; Turbulence measurements; Unsteady flow field

1. Experimental facility and instrumentation

The experimental investigations of the unsteady flow field have been conducted in the first stage of a two-stage low-speed axial compressor (NGAV). The compressor consists of an inlet guide vane and two repeating stages. It is operated in a closed system with atmospheric pressure because of its large dimensions. In addition to the advantage of less contamination in the compressor the construction with an integrated watercooler assures a constant fluid temperature during the experiments. The main design parameters are listed in Table 1. For more information see Traulsen (1989), Sentker and Riess (1996). Split-film probes with a radially oriented sensor have been attached to a mechanical traverse system and mounted at different axial positions on the low-speed axial compressor. With this traversing system an automatical positioning of the probes in radial and circumferential direction is possible. The split-film probes (Typ R57, Dantec) are operated in constant temperature mode with an overheat ratio of 1.7. They consist of two 3 μm nickel films deposited on a quartz fibre with 200 μm diameter and an active length of 1.25 mm. For the measurement of the unsteady velocity field in a turbomachine this probe type has the advantage of relatively small dimensions in circumferential direction and simultaneous acquisition of two components of the unsteady velocity vector in the 'S1-plane'. Frequencies up to 175 kHz can be measured.

2. Measurement procedure and evaluation method

For the measurements of the unsteady flow field in the first stage of the NGAV, a rotational speed of 2900 rev/min is chosen. The operating point is close to the design point with a total mass flow rate of 17.5 kg/s and a pressure ratio of $\Pi = 1.077$.

All investigations are conducted at 50% blade height. The probes have been traversed circumferentially in the axial gap in front of the first stator (E2), in four planes inside the stator blade row (E2a, E2b, E2c, E2d) and in one measuring plane behind the first stator (E3) which is indicated in Fig. 1. The stepping varied from 0.5° inside the stator blade row to 0.5–1° in the planes E2 and E3.

During the experiments a sampling rate of 200 kHz and a total measuring time of 2.62 s is chosen. This leads to a total number of 2^{19} single measured values at each measuring point.

A continuously recorded trigger, which is fixed to the rotor, enables a correct collection of the measured values into 4200 equidistant time windows – one window has the size of 4.926 μs per revolution. The samples in each time window are

* Corresponding author. Tel.: +49-511-762-2752.
E-mail address: sentker@ifs.uni-hannover (A. Sentker).

PII: S0142-727X(00)00011-4

Table 1
NGAV

Geometry			Design parameters		
Outer diameter	D_a	760 mm	Rotational speed	n_{nenn}	3000 rev/min
Chord length rotor	l_r	75 mm	Mass flow rate	$\dot{m}$	16.5 kg/s
Chord length stator	l_s	90 mm	Total pressure ratio	Π	1.07
Blade height	H	140 mm	Reynolds number rotor	Re_{LA1}	4.5×10^5
Number of rotor blades	z_r	30	Reynolds number stator	Re_{LE1}	4×10^5
Number of stator blades	z_s	26			

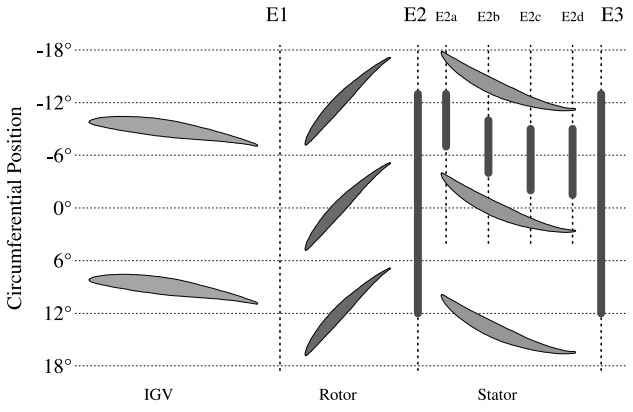

Fig. 1. Measuring planes in first stage.

ensemble averaged, which leads to 4200 values of $\vec{c}$ and $\overline{c_i'^2}$ for the 30 rotor pitches. An arithmetic averaging of the 30 rotor pitches in a phase locked mode delivers 140 values of $\vec{\bar{c}}$ and $\overline{\overline{c_i'^2}}$ 2 for an average rotor pitch (Sentker and Riess, 1997, 1998). In this paper only data for the average pitch are presented.

The absolute frame of reference for the evaluation of the mean square fluctuation components and an 'unresolved unsteadiness' calculated according to a formula normally referred to the turbulence intensity in macroscopically steady flows is the mainflow (subscript mf) and the crossflow (subscript cf) plane (Zaccaria and Lakshminarayana, 1997).

3. Experimental results and interpretation

3.1. Unsteady absolute velocity field

The unsteady velocity field in E2, E2b, E2d and E3 is presented in Figs. 2–5. In the three-dimensional plots the axis 'measuring position' means the probe position in the circumferential direction (see Fig. 1) and the axis 'rotor position' is the time axis related to the actual rotor position. A step of one degree rotor position corresponds to a time step of 57.47 μs.

The unsteady velocity field behind the rotor in E2, presented in Fig. 2, reveals three characteristics of the flow. Firstly the rotor wakes moving from the right to the left side diagonally through the flow field. They are characterised by a small velocity defect and a higher absolute velocity on the suction side of the rotor wakes. Secondly the downstream stator blades, too, exert an influence on the unsteady flow field behind the rotor. In the range of −9 to −4 and 6–11° measuring position the absolute velocity is about 5 m/s lower due to the potential effect exerted on the unsteady velocity distribution by the stator blades. Thirdly the wake of the IGV shows at 1.5° measuring position. It is responsible for the higher absolute velocity here (see Sentker and Riess, 1997).

In E2b (Fig. 3) the characteristic velocity distribution inside a stator channel shows a higher velocity near the suction side of the blade compared to the pressure side. The drop is about 12 m/s or 17.1% of the maximum velocity. In this measuring plane the diagonally moving rotor wake has a lower absolute velocity inside the wake compared to E2 but the increased velocity on the suction side has nearly disappeared.

The velocity gradient inside the stator channel from pressure side to suction side has decreased in E2d, where it is only

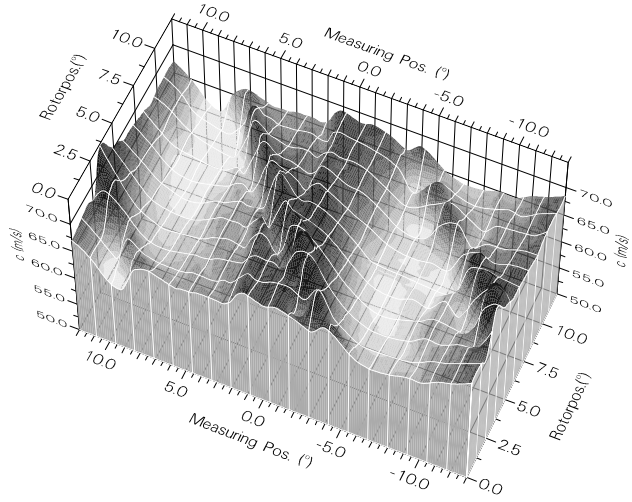

Fig. 2. Unsteady absolute velocity field in E2.

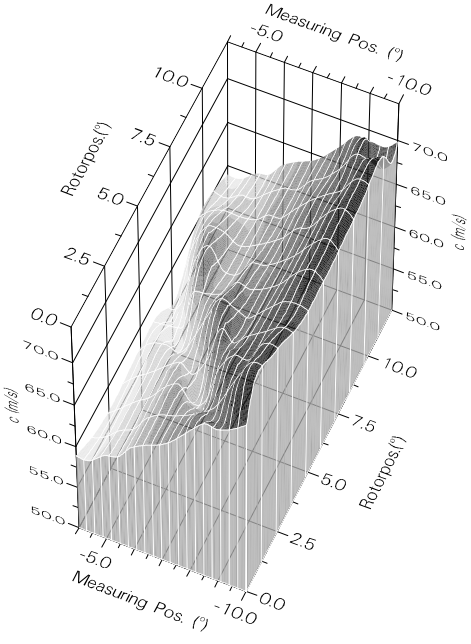

Fig. 3. Unsteady absolute velocity field in E2b.

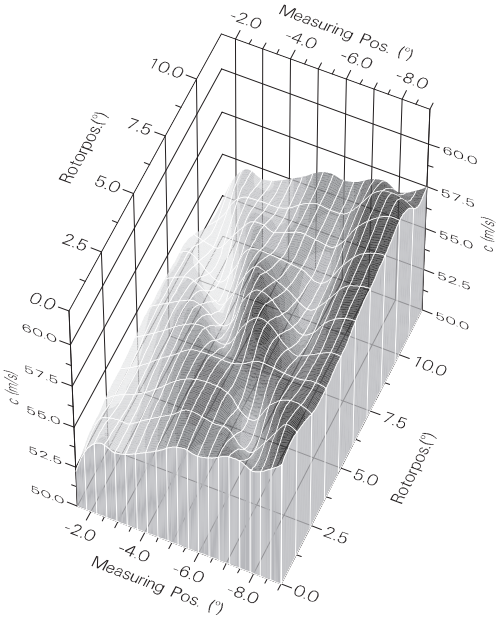

Fig. 4. Unsteady absolute velocity field in E2d.

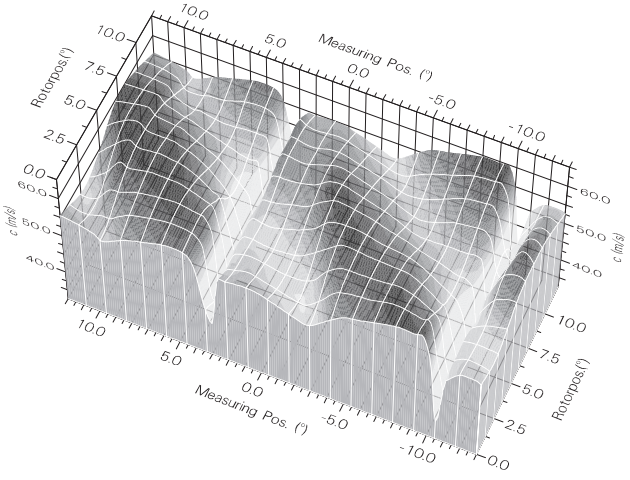

Fig. 5. Unsteady absolute velocity field in E3.

about 8.7% (see Fig. 4). The velocity defect due to the rotor wake can still be measured at this axial measuring position, but the minimum inside the rotor wake is lower.

Near to the suction side of the stator channel at $-7.5°$ measuring position, the absolute velocity increases suddenly. This abrupt increase indicates that not the pressure gradient inside the stator channel but the influence of the inlet guide vane, which was characterised by an increase of the absolute velocity in E2, is the reason for the higher velocity at $-7.5°$ measuring position.

Behind the stator in measuring plane E3 (Fig. 5) the unsteady velocity field is more complex with the additional disturbance caused by the wakes of the stator blades and the potential effect of the downstream second rotor. Spatially fixed at 3° and $-10.5°$ measuring position the wakes of the stator blades cause a strong decrease of the unsteady absolute velocity. Additionally, regions with a lower velocity moving diagonally through the diagram with a distance of 12°, that is one rotor pitch, can be seen. They are due to the potential effect of the downstream rotor and not the result of the upstream rotor wakes, because the spacing is very precise. The velocity defect due to the rotor wakes should be shifted by the velocity gradient inside the stator channel. The potential influence of downstream rotor prevails. This result will be proven in the following chapter by the presentation of the unsteady fluctuation components.

3.2. Turbulence intensity distribution in the first stage

The turbulence intensity, or unresolved unsteadiness, which is calculated from the mean square fluctuation components divided by the mean absolute velocity (Sentker and Riess (1997)), gives a good insight into the behaviour of the unsteady flow field travelling through the stator.

Considering the turbulence intensity in E2 (Fig. 6) most striking is the high turbulence in the wakes of the rotor blades with more than 4.5%. With a distance of 12° rotorposition they move from the right to the left side through the three-dimensional diagram. The wake of the IGV is also characterised by an increased turbulence intensity (2.5%). It is situated spatially fixed at 1.5–3° measuring position. At the position where the rotor and IGV wakes intersect the IGV wake is shifted, with the part on the suction side of the rotor wake moving faster than that on the pressure side. Inside the stator channel in E2b presented in Fig. 7 the rotor wake is still visible due to its high turbulence intensity of 4%. The shape of the rotor wake is changing inside the stator channel. The absolute velocity near the suction side of the channel is higher so that the part of the rotor wake near to the suction side of the channel is transported faster downstream. This results in a twisting of the rotor wake in the three-dimensional diagram. Near the pressure side of the stator channel occurs a spatially fixed region with a higher turbulence intensity. It can be assumed that the increased turbulence at this measuring position results from an IGV wake. Changing the operating point of the compressor leads to other positions of this region of increased turbulence inside the stator channel. This fact underlines, that the higher turbulence near the suction side of the stator channel is not generated by the velocity or pressure distribution inside the stator channel but originates from the IGV wake.

Considering Fig. 8, where the turbulence intensity in E2d is shown, supports the observation that an influence of the IGV wake on the unsteady flow field is still detectable there. In a measuring range of 60° to $-7.5°$ a spatially fixed region with increased turbulence intensity is visible, which can be identified as the IGV wake. Compared to the absolute velocity

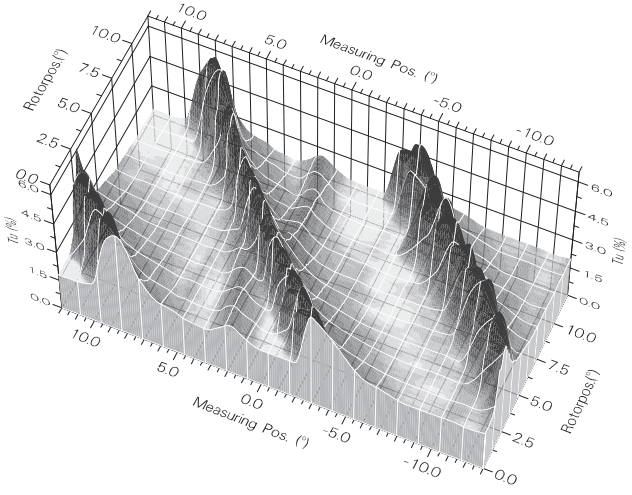

Fig. 6. Turbulence intensity distribution in E2.

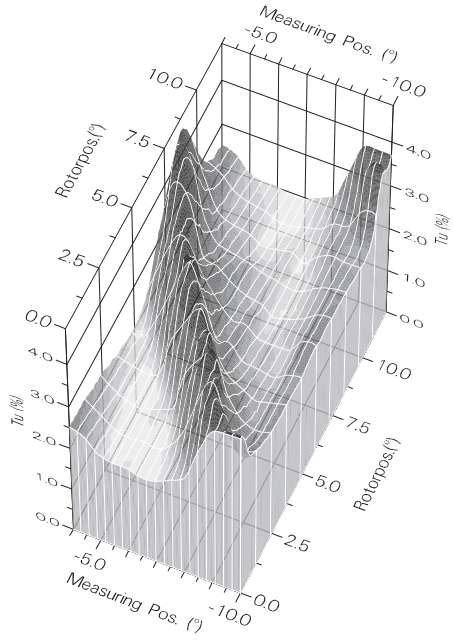

Fig. 7. Turbulence intensity distribution in E2b.

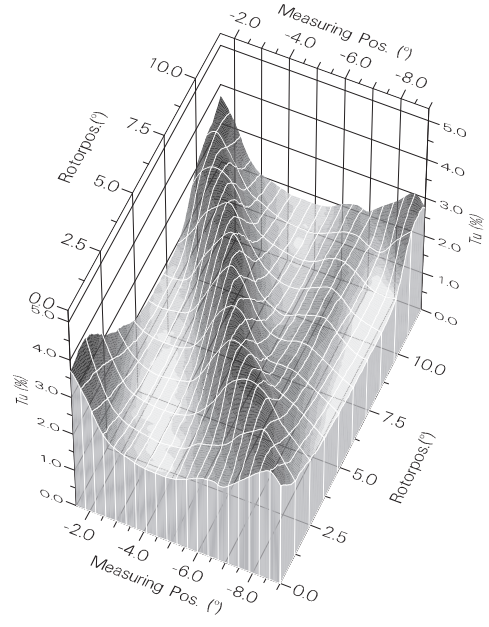

Fig. 8. Turbulence intensity distribution in E2d.

distribution the position of the IGV wake has changed, because the highest turbulence occurs inside the wake and the max. velocity in Fig. 4 comes from the suction side of the IGV wake. The maximum turbulence inside the rotor wake in E2d is with 3.5% lower than in E2b with 4.5%. In the measuring plane behind the stator, presented in Fig. 9, the wakes of the stator with a turbulence intensity of about 9% are dominant. They are spatially fixed at 3.5° and −10.5° measuring position. In contrast to Fig. 5 the diagonal regions with an increased turbulence level are the wakes of the upstream rotor, transported through the stator. The time distance between two adjacent rotor wakes is no longer constant at 12° but has diminished. The wakes are shifted clockwise due to the velocity gradient inside the stator pitch.

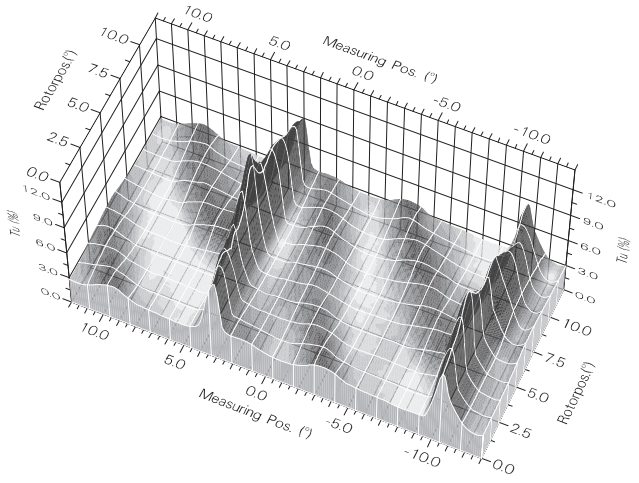

Fig. 9. Turbulence intensity distribution in E3.

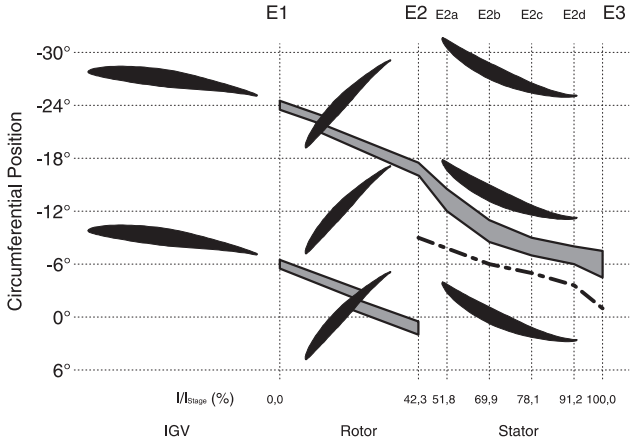

Fig. 10. IGV wake in first stage.

Considering the position of the interaction between stator and rotor wake, a difference of 6° rotor position between the part of the rotor wake on the suction side compared to the part on the pressure side of the stator wake can be determined. Near the pressure side of the stator wake the curvature of the rotor wakes is strong.

The IGV wake, too, is weakly visible at −4.5° to −7.5° measuring position. The increase of the turbulence intensity due to the IGV wake is not very strong behind the stator. It has been nearly mixed out.

In Fig. 10 the way of the IGV wake through the first stage is reconstructed schematically from the measured unsteady flow data. The extension in circumferential direction in E2a and E2b could not be measured because the IGV wake is situated at the border of the max. possible probe traverse. The IGV wake follows an imaginary streamline on its way through the stator. Its circumferential extension grows from E2 to E3, it follows the curvature of the stator blade.

3.3. Fluctuation components in first stage

The decay of the undisturbed rotor wake during the passage through the stator can be shown by selecting sections through the three-dimensional diagrams at times (i.e. rotor positions), when the rotor wake is in the middle of the stator channel. The dotted line in Fig. 10 indicates the actual rotor wake positions

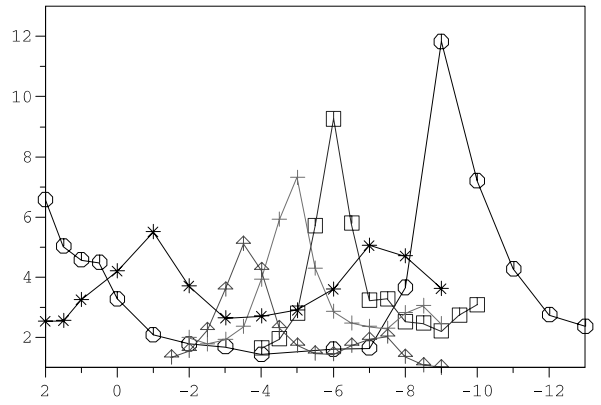

Fig. 11. Mean square fluctuation components in mainflow direction.

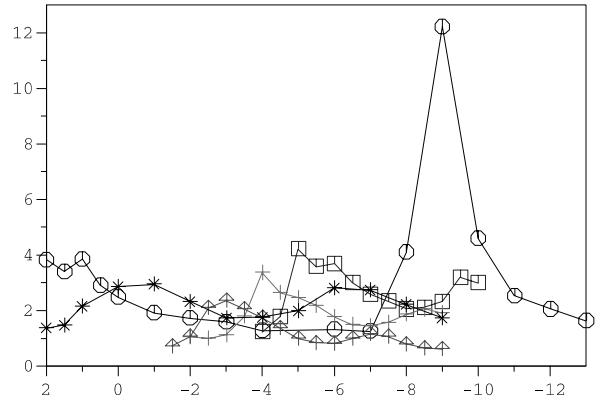

Fig. 12. Mean square fluctuation components in crossflow direction.

chosen for the detailed examination of the unsteady flow components within the stator in Figs. 11 and 12. These positions are chosen because there neither the side walls nor the IGV wake exert an influence on the rotor wake. The evaluation of the absolute fluctuation components avoids the reference to – and thus the influence of – the varying velocity level through the stator, as this per definition is the case for the turbulence intensity.

In Fig. 11 the mean square fluctuation components in mainflow direction $\overline{c'^2_{mf}}$ of the selected sections are plotted over the measuring position for all measuring planes. In E2 the fluctuations in mainflow direction in the rotor wake reach the highest value with 12 m^2/s^2. The fluctuations in the rotor wake decrease continuously down to E2d with 5.2 m^2/s^2 and increases slightly again in E3. In the undisturbed regions outside of the rotor wake the minimum value of the fluctuations in mainflow direction is nearly constant with little more than 2 m^2/s^2 in all measuring planes from E2 to E2d, it increases to 3 m^2/s^2 in E3 behind the stator.

In the measuring planes E2b to E2d the mean square fluctuations in mainflow direction $\overline{c'^2_{mf}}$ show a smaller second maximum near the suction side of the channel due to the wake of the IGV. An increase in E2d near the pressure side of the channel is not fully understood yet.

Considering the development of the mean square fluctuations in crossflow direction $\overline{c'^2_{cf}}$ presented in Fig. 12 they are of the same level as the longitudinal fluctuations within the rotor wake in plane E2. Remarkably they decrease in the rotor wake from E2 to E2b by about 65% to 4% m^2/s^2. The decrease

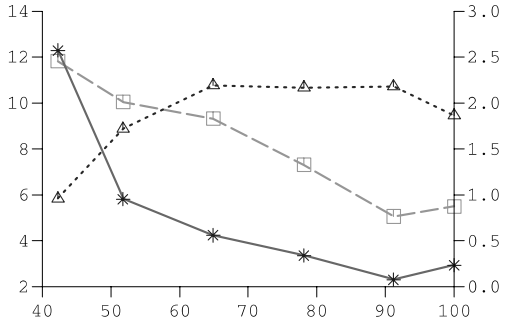

Fig. 13. Maximum of fluctuation components.

continues to E2d, where 2.3 m^2/s^2 are reached. Additionally the shape of the rotor wake changes. The decrease of $\overline{c'^2_{cf}}$ on the suction side of the rotor wake is smoother, the wake becomes broad. The fluctuation components in crossflow direction in E2b and E2c are higher near the suction side of the stator channel, too, due to the IGV wake, but no increase towards the pressure side is detectable.

Fig. 13 shows the maximum values of the fluctuation components inside the rotor wake over a non-dimensional length scale l_{stage}/l_{axial}. Behind the rotor the unsteady flow field inside the rotor wake is nearly isotropic, with $\overline{c'^2_{mf\,max}} = \overline{c'^2_{cf\,max}}$. Entering the stator channel the fluctuations in crossflow direction decrease exponentially whereas the fluctuations in mainflow direction decrease linearly. The plot of the ratio $\overline{c'^2_{mf\,max}}/\overline{c'^2_{cf\,max}}$ underlines this phenomenon. It increases from 1 to 2.2 and remains constant for the rest of the stator channel.

The description presented here of the decay of the fluctuation components in the rotor wake through the stator by measurements at different axial positions and time instants is open to a number of criticisms in detail. For example it cannot be ensured, that the maximum of the wake has always been captured. Therefore the stepping of the probe in circumferential direction has to be diminished. Additionally a comparison with measurements at other operating points of the compressor would be helpful in order to give a more general impression of the wake decay. But, as other investigations have shown, the comparison with the results at other time steps is consistent with the results presented here, only the absolute range of the values is slightly changing.

4. Conclusions

This paper gives details of the unsteady absolute velocity field and the turbulence field mid plane at 50% blade height of the first stage of a two stage low-speed axial compressor. At six different axial positions in front of, inside and behind the first stator the unsteady flow field has been examined in space and time. In detail it shows:

1. the IGV wake moving through the stator blade row. It is situated at spatially fixed positions, following the curvature of the stator blade. The turbulence intensity in the IGV wake decreases slightly and the wake becomes broader, but is not fully mixed out behind the stator;
2. the characteristics of the rotor wakes at different axial positions within and behind the stator blade row. The rotor wake is shifted clockwise inside the stator blade row due to the velocity gradient between the suction and the pressure side of the channel. The turbulence intensity in the rotor wake decreases on the way through the stator, the longitudinal and the lateral fluctuations show a distinctly different decay mode.

Acknowledgements

The Deutsche Forschungsgemeinschaft (DFG) supported the construction of the low-speed axial compressor (NGAV) in the program SFB 211. The authors want to express their sincere gratitude.

References

Sentker, A., Riess, W., 1996. In: Rodi, W., Bergeles, G. (Eds.),Turbulence Intensity Measurements in a Low Speed Axial Compressor, Engineering Turbulence Modelling and Experiments 3, Elsevier, Amsterdam, pp. 773–783.

Sentker, A., Riess, W., 1997. Unsteady flow and turbulence in a low speed axial compressor. In: Eighth International Symposium on Unsteady Aerodynamics and Aeroelasticity of Turbomachines, 15–18 September. Stockholm.

Sentker, A., Riess, W., 1998. Measurement of unsteady flow and turbulence in a low speed axial compressor. Experimental Thermal and Fluid Science 17, 124–131.

Traulsen, D., 1989. Axialverdichterprüfstand zur Untersuchung von Randzonenströmungen, Fortschrittberichte VDI, Reihe 7, Nr. 161.

Zaccaria, M.A., Lakshminarayana, B., 1997. Unsteady flow field due to nozzle wake interaction with the rotor in an axial flow turbine: part I rotor passage flow field. Journal of Turbomachinery 119, 201–213.